© Universiti Tun Hussein Onn Malaysia Publisher's Office

IJIE

Journal homepage: http://penerbit.uthm.edu.my/ojs/index.php/ijie
ISSN : 2229-838X e-ISSN : 2600-7916

International Journal of Integrated Engineering

Durability Map for The Friction Stir Welding Tools with Flat Faced Pins

Stephen Leon. J[1*], Bharathiraja.G[1], Jayakumar.V[2]

[1]Department of Mechanical Engineering, Saveetha School of Engineering, Saveetha Institute of Medical and Technical Sciences, Chennai, Tamilnadu, INDIA

[2]Department of Mechanical Engineering, Amrita School of Engineering, Amrita Vishwa Vidyapeetham, Chennai, Tamil Nadu, INDIA

*Corresponding Author

DOI: https://doi.org/10.30880/ijie.2020.12.08.008
Received 21 February 2020; Accepted 10 April 2020; Available online 30 August 2020

Abstract: In friction stir welding, tools made with flat faced pins deliver comparatively higher strength joints than circular pins. However, its non-axisymmetric cross section about the rotational axis results in fluctuating stress along its surface that leads to premature tool failure. This requires a systematic definition for process parameter selection domain based on the number of flat faces in the pin to improve tool life. Temperature dependent strength of the material to be joined in the stir zone is the only source of opposing force for the tool movement. To predict opposing force, temperature gradient developed by the different levels of process parameters in the stir zone is numerically quantified with an experimentally validated model. Based on the estimated temperature, maximum stress acting on the tool pin is quantified with a remodified temperature dependent analytical model. The effect of increase in process temperature on the strength of the weld joint is experimentally analyzed through the investigation of change in hardness value in heat affected zone. Obtained results are used to develop tool durability maps for tools with flat faced pin in a domain on which higher and lower limits are fixed by considering satisfactory level of joint strength and tool life respectively. These maps provide flexibility in the parameter selection with an acceptable level of compromise in joint strength or in tool life based on the quality requirement of weld joint.

Keywords: Friction stir welding, non-circular tool pin, tool life, durability map, force, principal stress

1. Introduction

In friction stir welding, entire process depends on the heat generated by the relative motion between the workpiece and tool. Tool experiences three different stages plunge, dwell and welding as shown in Fig. 1. Since in all these stages workpiece is maintained in solid state, the tool is exposed to large amount of opposing force during its movement along the weld line. This resistance force given by the parental metal causes mechanical erosion [1] in the tool.

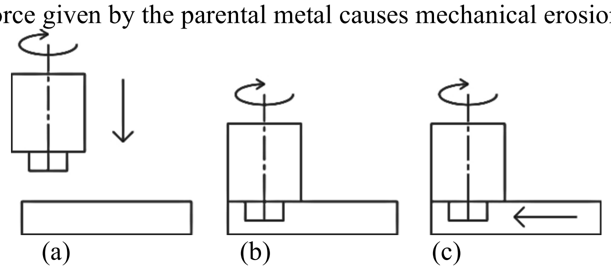

Fig. 1 - Classification of FSW process: (a) plunging; (b) dwelling; (c) welding

*Corresponding author: stephenleonj@gmail.com

Among all the parts pin is the weakest part in the tool. As it is completely submerged inside the workpiece, it experiences comparatively higher stress. So tool durability in friction stir welding for the given working environment completely depends on the ability of the tool pin to withstand maximum stress produced during the process. Non- circular design in the tool pin proved enhanced post weld properties [2, 3], but it is not widely used like circular design due to its premature failure during the process.

Various modifications were done in the non-circular pin design to reduce the stress experienced by the pin surface during the process. Truncated cone probe with stepped spiral could withstand huge traverse force [4, 5] which is suitable to operate the tool with high strength materials. Although this design is compatible for higher traverse force, failure is caused due to the moment produced in its thinner base. Lesser static volume of the whorl probe comparing with its dynamic volume during rotation reduces material displacement up to 60% [6]. This reduction in quantity of material displacement helps to increase the feed rate during the process and make the whorl design suitable for higher speed friction stir welding. Whorl probe with helical ridge on its surface enhances the downward motion of the material in the stir zone [7] which reduces the void formations in the weldment. These whorl probes were remodified with flute cuts in its helical ridge which further reduced the material displacement up to 70% [4] and also this modification increased the contact surface area of the tool/matrix interface. Increase in contact surface area increases the heat generation rate. This improvised design made it possible to weld up to 75mm thick AA6082-T6 plates [8, 9].

Although reduction in material displacement reduces traverse force on the usage of Whorl probes, its complex surface design resulted material entrapment during the rotation which caused higher shear stress in the probe. This problem was eliminated by trivex shape probe [10] by which over 12% reduction in forging force in advancing side was achieved. Further studies by Clogrove et al. [10] proved that triflat pin produced better post weld properties than triflute and trivex profiles. Various experiments [11, 12] done with different polygonal shaped pin probes exhibit comparatively superior weld quality than other tools with non-circular pin shapes.

Difficulty in the manufacturing of complex probe profiles like triflute and trivex and the nature of delivering better post weld properties suggest the usage of polygonal shaped non-circular pins in the tool although stress experienced by this design is comparatively more. Traverse force experienced by the pin depends on the process temperature as the workpiece material's shear strength is reduced in the elevated temperature. So tool durability depends on the process temperature dependent workpiece material property. Exact estimation of temperature dependent torque produced in the tool pin for the given polygonal shape helps to optimise process parameters to enhance the tool life.

Maximum stress produced in the pin was estimated by Arora et al.[13] through the assumption of pin as a short cantilever beam. It was concluded that the maximum shear stress in the tool pin is almost equal to the shear strength of the parental metal to be joined with respect to the process temperature. Based on this methodology Mehta et al. [14] analysed torque, traverse force and bending moment acting on the non-circular shaped pin. In subsequent studies, Mehta et al. predicted maximum principle stress at various points in the tool pin surface as a combined effect of torque, traverse force and bending moment. Apart from the analytical solutions many experimental researches [15] have proved that force acting on the tool is directly affected by the dimension and geometrical shape of the tool pin.

From the analytical models and experimental results, it is evident that increase in tool durability depends on the reduction in shear strength of the material to be joined which can be achieved through the increase in process temperature. But increase in process temperature enlarges heat affected zone which eradicates the post weld properties of joined material. This necessitates an optimisation in process temperature based on the pin shape, pin dimensions, temperature dependent tool and material properties.

In this paper, a novel analytical model is developed to estimate the torque produced along the pin flat surfaces. This analytical model is used to remodify the existing analytical model to estimate the principal stress acting on various points along the pin surface to quantify the maximum principal stress developed in the prescribed location. As the force developed by the material against tool movement depends on temperature of the material in the stir zone, a numerical model is developed to identify the temperature gradients developed during the process in the stir zone. This numerical model is validated through experiments conducted on various levels of process parameters. Based on the obtained results, temperature dependent tool and material strengths are estimated and corresponding tool index number is quantified through the analytical estimation of maximum principal stress. Apart from these, the effects of temperature raise on the joint strength are identified through the experimental investigation of hardness distribution at various points of the weld joint. Considering the satisfactory level of tool life and joint strength, a process temperature domain is defined based on the tool pin shape. Tool durability map is prepared in this domain.

2. Analytical modeling

Tool experiences opposing force for its traverse motion along the weld line, in addition to the rotating torque as shown in Fig. 2. Due to these forces, being a weaker component, tool pin experiences severe stress and undergoes wear. Tool durability depends on the ability of the pin to withstand the maximum stress. So the tool index can be defined through the analysis of traverse force, shear stress and torque experienced by the pin during the joining process. Experimental measurement of stresses acting on the pin is impractical as it is totally submerged inside the workpiece during the process. So the combined effects of torque produced during rotation, shear stress and bending moment during the forward motion can be estimated analytically.

Fig. 2 - Torque exerted by one tool pin segment and tool shoulder

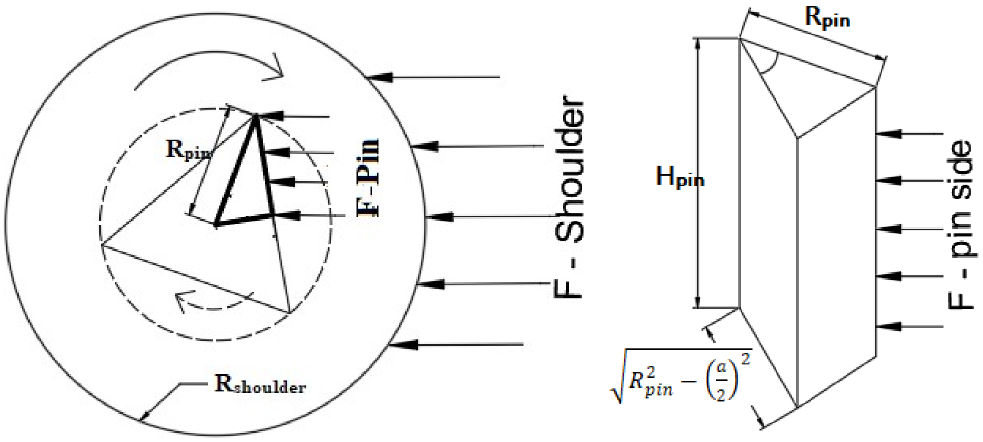

Tool pin undergoes both sliding as well as sticking torque during its relative motion with respect to the workpiece.

$$T_{Total} = T_{sticking} + T_{sliding} \tag{1}$$

Which can be obtained by [16],

$$T_{Sliding} = \oint_{A_{pin-side}} \delta\mu\sigma dA + \oint_{A_{pin-tip}} \delta\mu P dA \tag{2}$$

$$T_{Sticking} = \oint_{A_{pin-side}} (1-\delta)\tau dA + \oint_{A_{pin-tip}} (1-\delta)\tau dA \tag{3}$$

Where δ is fractional slip and μ is friction coefficient is given by [17],

$$\delta = 0.31 \exp\left(\frac{R_{Shoulder}\omega}{1.87}\right) - 0.026 \tag{4}$$

$$\mu = 0.5 \exp(-\delta R_{Shoulder}\omega) \tag{5}$$

and ω is tool rotational speed, a is the pin side length, P is vertical force, σ is yield stress and τ represents shear yield stress and is given by,

$$\tau = \frac{\sigma}{\sqrt{3}} \tag{6}$$

Considering the continuously varying boundaries of the pin, torque developed along the horizontal contact surface of the pin can be estimated by [18]

For triangular shape,

$$T_{Pin\text{-}tip} = \frac{2\pi(1-\delta)\tau a^3}{9\sqrt{3}} \tag{7}$$

For Square shape,

$$T_{Pin\text{-}tip} = \frac{\pi(1-\delta)\tau a^3}{3\sqrt{2}} \tag{8}$$

In these equations sticking torque alone considered [14].

In order to estimate torque produced along the vertical surface of the pin, irrespective of the pin shape, it is divided into small triangular prism shaped segments as shown in fig. Torque produced along the vertical surface of one segment can be estimated by,

$$T_{pin\text{-}side} = \oint_{A_{pin-side}} (1-\delta)\tau dA \tag{9}$$

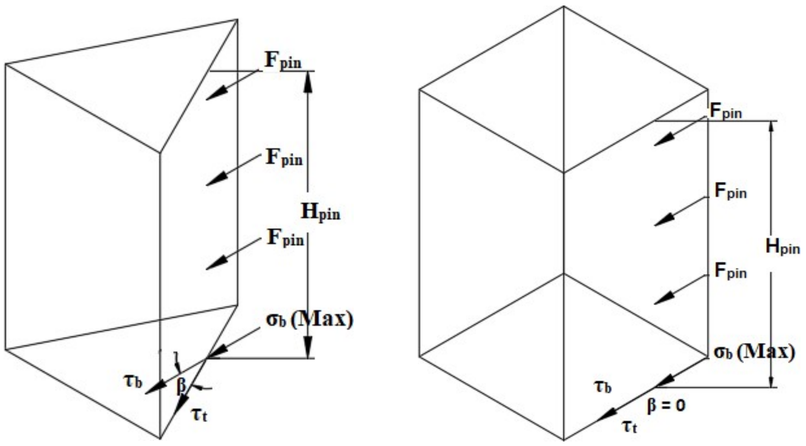

(a) (b)

Fig. 3 - Stress components in (a) triangular pin and (b) square pin

From Fig. 3, it can be concluded as,

$$A_{pin\text{-}side} = f(H,r)\begin{cases}\sqrt{R_{pin}^2-\left(\frac{a}{2}\right)^2}\le r\le R_{pin}\\ 0\le H\le H_{pin}\end{cases}$$

Traverse force experienced by the vertical surface of the one segment is,

$$T_{pin\text{-}side} = (1-\delta)\tau\int_0^{H_{pin}} dH \int_{\sqrt{R_{pin}^2-\left(\frac{a}{2}\right)^2}}^{R_{pin}} r\,dr$$
$$= (1-\delta)\tau\frac{a^2}{8}H_{pin} \quad (10)$$

Considering the total number of segments (six segments for triangular shape and eight segments for square shape) in the tool pin, this equation can be remodified as,

For triangular shape,

$$T_{pin\text{-}side} = \frac{3}{4}(1-\delta)\tau a^2 H_{pin} \quad (11)$$

For square shape,

$$T_{pin\text{-}side} = (1-\delta)\tau a^2 H_{pin} \quad (12)$$

Pin experiences normal stress due to bending (σ_b), shear stress due to bending (τ_b) and shear stress due to torsion (τ_t). The value of stress increases gradually from the pin root to tip. As the tool life depends on the point at which it undergoes maximum stress, for the current analysis stress at the tip of the tool pin alone is considered.
Maximum stress due to the bending at the tip of the pin for both triangular and square shape is given by,

$$\sigma_b = \frac{X}{I_{yy}}\int_0^{H_{pin}} F_{pin} h\,dh \quad (13)$$

Maximum shear stress acting at the tip of the pin is given by [18],
For triangular shape,

$$\tau_b = \frac{32L}{a^4\sqrt{3}}\left(\frac{\sqrt{3}aX}{2}-X^2\right) \quad (14)$$

For square shape,

$$\tau_b = \frac{12L}{a^4}\left(\frac{aX}{2}-\frac{X^2}{2}\right) \quad (15)$$

In these equations, bending force acting on the vertical surface of the pin (F_{pin}) and shear force acting at the tip of the pin (L) is equal to the temperature dependent shear strength ($\tau(t)$) of the material [13]. X represents the distance of the point in the segment where the maximum stress acts (ref fig.3). I_{yy} is the moment of inertia for the shape to be estimated. Applying all these values for the triangular and square geometries, the equations (13, 14 & 15) can be consolidated as,

For triangular pin,

$$\sigma_b = \frac{8F_{pin}H_{pin}}{a^3} \tag{16}$$

$$\tau_b = \frac{2\sqrt{3}V}{a^2} \tag{17}$$

and shear stress due to the rotational torque for triangular section is given by [14],

$$\tau_t = \frac{20T_{pin}}{a^3} \tag{18}$$

For square pin,

$$\sigma_b = 0 \text{ at the point where maximum principal stress exist} \tag{19}$$

$$\tau_b = \frac{3V}{2a^2} \tag{20}$$

and shear stress due to the rotational torque for triangular section is given by [14],

$$\tau_t = \frac{T_{pin}}{0.208a^3} \tag{21}$$

The resultant maximum stress experienced by the pin is obtained by,

$$\tau_{max} = \sqrt{\left(\frac{\sigma_b}{2}\right)^2 + (\tau_b + \tau_t\cos\beta)^2 + (\tau_t\sin\beta)^2} \tag{22}$$

Here, β is the angle between τ_b and τ_t which is equal to 30° for triangular pin and 0° for square pin (Ref. Fig. 3). In these equations, shear strength of the material depends on the temperature experienced by the material in the stir zone during the joining process. As the process during welding stage is done on the steady state, properties can be taken for the observed steady state temperature gradient.

3. Numerical modelling

Force given by the material on the tool surface drastically reduces when there is an increase in temperature of the material approaching the tool surface. So **s**tress developed on the surface of the tool pin is completely dependent on the temperature in the stir zone. Experimental measurement of temperature rise along the tool pin/matrix contact surface during the process is highly challenging. So a transient thermal model is developed to estimate the temperature at various points in the stir zone. Heat input for the numerical model is calculated through the analytical heat generation model in which total heat generation is estimated by [12],

$$Q_{Total} = \frac{2}{3}\pi\tau_{contact}\omega(R^3_{shoulder} + X.R^2_{pin}H_{pin}) \tag{23}$$

Where multiplication factor X depends on the shape of the tool pin. X = 0.72 for triangular and X= 0.95 for square pin. In this equation total heat supply is attained through the summation of heat supplied by the shoulder, pin tip and pin side interfaces with the matrix. It can be calculated by [12]

$$Q_{pin\text{-}tip} = \frac{2}{3}\pi\tau_{contact}\omega R^3_{pin}$$

$$Q_{pin\text{-}side} = 2\pi\tau_{contact}\omega R^2_{pin}H_{pin}$$

$$Q_{Shoulder} = \frac{2}{3}\pi\tau_{contact}\omega R^3_{shoulder} - Q_{pin\text{-}tip}$$

From the analytical models, it is clear that,

$$Q_{Total} = f(R_{Shoulder}, R_{pin}, H_{pin}, P, \omega)$$

So in order to analyse the influence of all the direct and indirect influencing variables, various levels of different parameters are selected for the current analysis (Ref. Table 1). Increase in weld velocity reduces the effective heat supply. Effective heat supply $Q_{eff} = Q_{Total}$ / weld velocity. Values of effective heat supply for every trail based on the chosen weld velocity is listed in Table 3

Table 1 - Levels of process variables for friction stir welding on AA2024-T3

Parameter ID	Parameter	Levels			
		0	1	2	3
A	Shoulder radius/pin radius $R_{shoulder} / R_{pin}$	2.5	3	3.5	4
B	Tool rotation speed (rpm)	800	1000	1200	1400
C	Vertical Pressure, P (kN)	7	8	9	10
D	Weld velocity, V (mm/sec)	1.67	1.83	2	2.17

Table 2 - Tool dimensions

Pin profile ID	No.sides in tool pin (n)	Tool pin circumferential diameter (mm) D_{pin}	Tool pin side length (mm) (a)	Tool pin height (mm) H_{pin}	Tool shoulder diameter (mm) $D_{Shoulder}$			
					Tool 1	Tool 2	Tool 3	Tool 4
T	3	6	5.2	5.6	15	18	21	25
S	4	6	4.2	5.6	15	18	21	25

Table 3 - Mechanical and thermal properties [19]

Property/parameter	Work piece (AA2024-T3)	Tool (H13)	Backing plate (Mild steel)
Thermal conductivity (W/mK)	151	20.5	51.5
Specific Heat capacity (J/Kg K)	875	510	425
Density (Kg/m^3)	2780	8150	7800

Table 4 - Analytical heat input values for different trails

Trial No.	Tool used (ID)	Design matrix				Effective heat supplied (J/mm)
		A	B	C	D	
1.	T1	0	0	0	0	369
2.	T2	1	1	1	1	578
3.	T3	2	2	2	2	867
4.	T4	3	3	3	3	1292
5.	S2	1	3	3	3	589
6.	S1	0	2	2	4	611
7.	S4	3	1	1	1	893
8.	S3	2	0	0	2	797

3.1 Initial and boundary conditions

Heat input boundaries:

$$K\frac{\partial T}{\partial n} = Q_{Total} \begin{cases} Q_{Shoulder}, & R_{pin} \leq R \leq R_{Shoulder} \\ Q_{Pin-tip}, & 0 \leq R \leq R_{pin} \\ Q_{Pin-Side}, & 0 \leq h \leq H_{pin} \end{cases}$$

Heat dissipation boundaries:

Backing plate:

$$K\frac{\partial T}{\partial n} = Q_{Conduction} \begin{cases} y = b \\ -w \leq x \leq w \end{cases}$$

Other boundaries:

$$K\frac{\partial T}{\partial n} = h_x(T_x - T_{amb})$$

Here, T_x is the temperature at any point exposed to the atmosphere, h_x and T_{amb} is the heat transfer coefficient and temperature of the surrounding air, w is the width of the plate, b is the thickness of the plate and K is the thermal conductivity of the workpiece material. Heat transfer coefficient (h_x) is assumed as 100 W/mk and ambient air temperature considered as 27 $^{\circ}$C

Initial temperature = 27 at all the points of the tool, workpiece and backing plate. Other mechanical and thermal properties of tool and workpiece materials are given in Table 3.

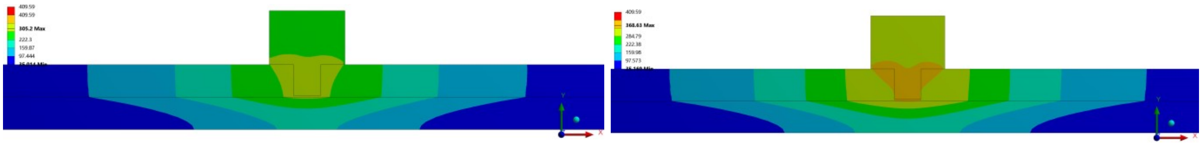

(a) Trail no.1 **(b) Trail no.2**

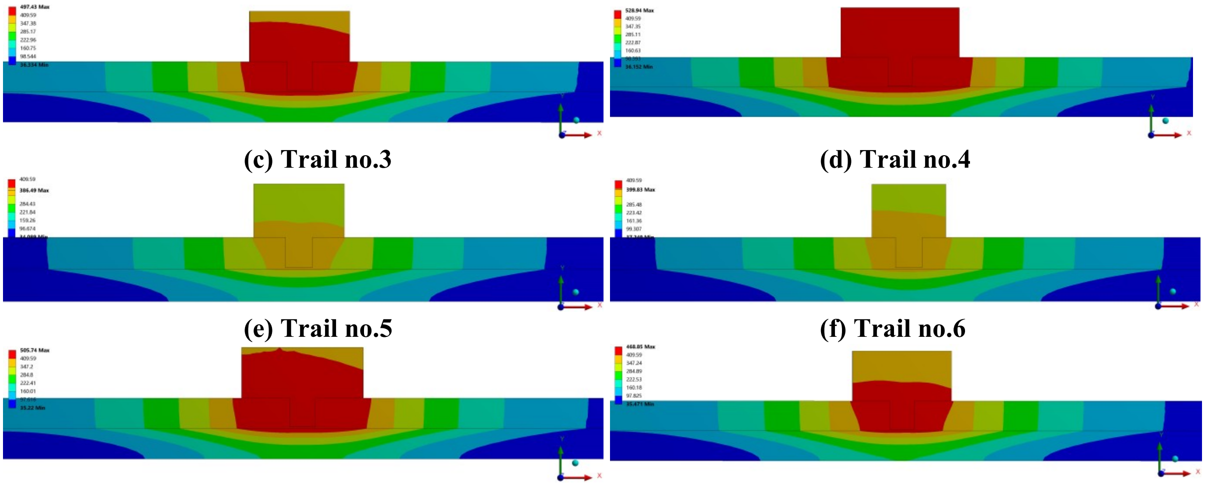

(c) Trail no.3 **(d) Trail no.4**

(e) Trail no.5 **(f) Trail no.6**

(g) Trail no.7 **(h).Trail no.8**

Fig. 4 - Temperature distribution during welding stage

4. Experimental analysis

The major purpose of conducting experimental study is to optimise the process parameters which has direct and indirect influence on maximum temperature raise during welding. This will help to identify a balanced range of working temperature which causes lesser effects on mechanical properties in the heat affected zone without compromising tool life. Friction stir welding was carried out in AA2024-T3 plates (300mm X 150mm X 6mm) using HURCO VMX24 machine centre. In order to analyse the effects of tool geometries and dimensions, eight different tools were manufactured using H13 tool steel as per the details given in Table.2. To understand the expanded range of heat affected zone hardness test was conducted at various points in the increasing distance from the weld centre both in advancing and retreating sides of joined workpieces. Apart from the heat affected zone analysis, in the view of validating the temperature obtained from the numerical model, two thermocouples (TC_1 and TC_2) were placed at the edge of the stir zone as shown in Fig. As the shoulder radius on every trail is different, the locations of thermocouples are adjusted in such a way that its distance from the stir zone is equal to 0.4mm.

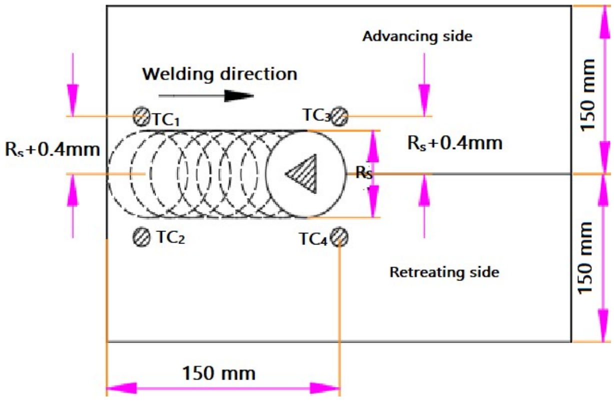

Fig. 5 - Layout of the experimental setup

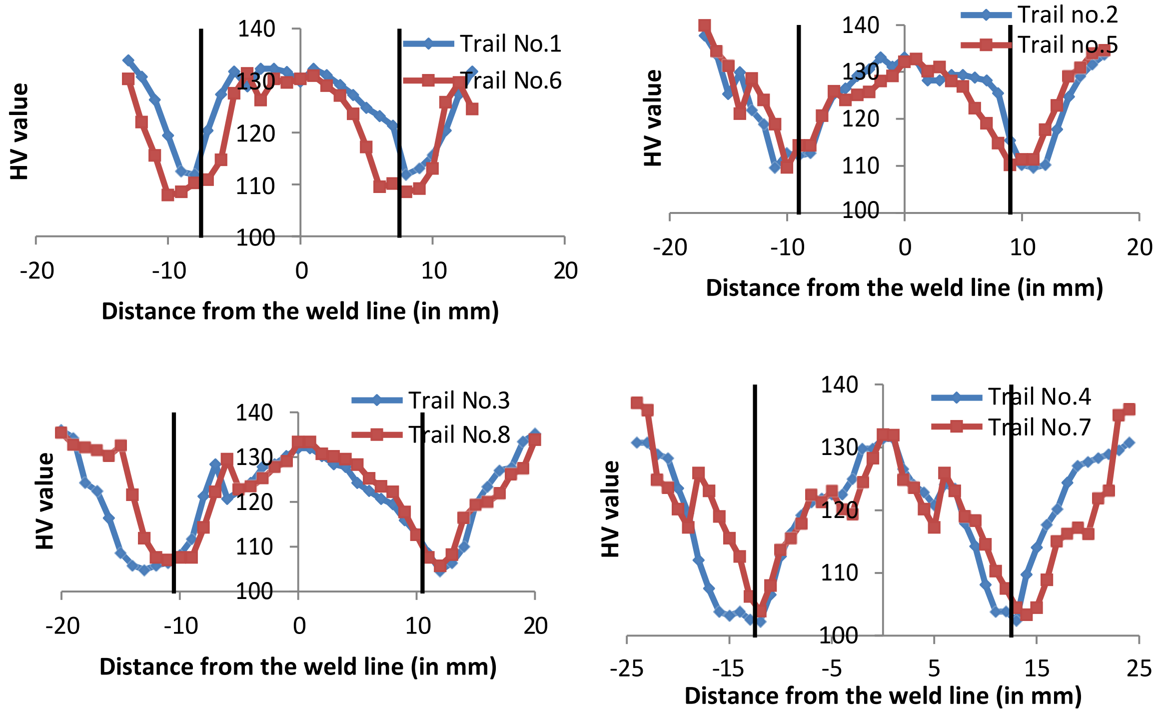

Fig. 6 - Distribution of hardness values

5. Results and Discussions

5.1. Material strength response to the process thermal history

Fig.4 indicates the numerically obtained temperature distribution at various points during the process. Maximum temperature attained under the shoulder in Stir Zone (SZ) and the corresponding temperature raise in other points of SZ and Heat affected zone (HAZ) depends on the levels of process parameters chosen for the trail. When the temperature of Aluminium alloy 2024-t3 reaches 410 (80% of its solidus temperature, T_s), it drastically loses its strength and becomes soft plasticised material [16]. This soft region is denoted in red colour in Fig.4. In order to analyse the tool durability during low heat joining processes, few trails (Trail no. 1, 2, 5 & 6) are performed under 410 (less than $0.8T_s$).

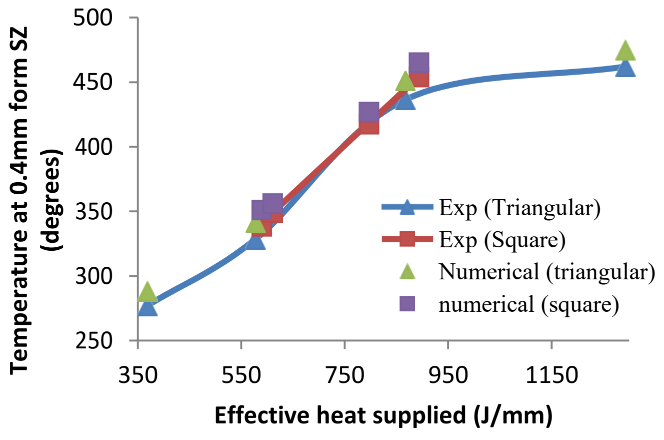

Fig. 7 - Experimental validation of thermal history

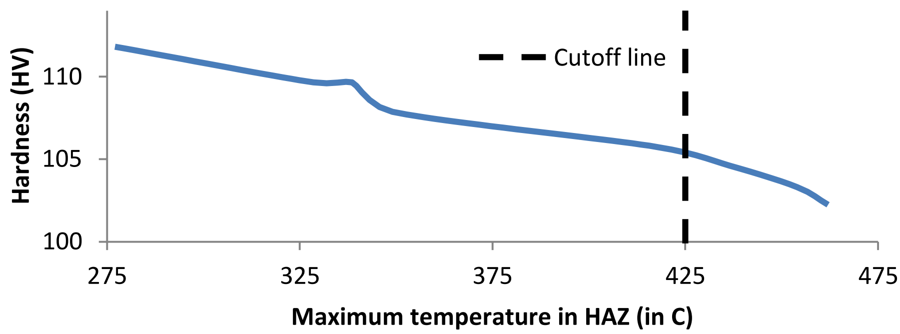

Fig. 8 - Change in Hardness values with respect to temperature rais

From the obtained models it is clear that expansion of HAZ in every trail highly depends on the shoulder radius irrespective of the pin shape. So, shoulder is the major contributor in heat generation. A comparative analysis has been exhibited in Fig.7 between the experimentally and numerically attained temperature values at the edge of the tool shoulder to validate the proposed model. The point for this analysis is taken at a distance of 0.4mm from the shoulder radius. Average between the temperature readings of TC_1 and TC_2 was taken as experimental values in Fig.7 to consider the temperature difference between the advancing and retreating sides. It can be observed from the numerical model in Fig.4 when the ratio of shoulder and pin radius lesser than 3.5, there is considerable difference in temperature gradients form the shoulder towards the bottom of the workpiece in the SZ. As the strength of the material depends on the temperature, it can be noted that the strength of the material increases forms the root to the tip of the pin considerably.

When the process variable levels are selected to increase the temperature in SZ, it results in increase of tool life. But increase in temperature beyond its restructure temperature leads to local dissolution of strengthening particles in aluminium alloys during friction stir welding in HAZ. Thermal cycles produced during the joining process causes aging and recovering process in HAZ both in advancing and retreating sides [20]. When the peak temperature of these cycles increase, it reduces the hardness both in HAZ and SZ. Fig.6 explains the change in hardness values in HAZ with respect to the temperature. Irrespective of process variables and process peak temperature almost all the trails exhibits minimum values hardness in the beginning of HAZ and at the end of the Thermo-mechanically affected zone where the metal grains are affected only because of the temperature raise. Although the temperature raise in SZ is comparatively higher than HAZ, the hardness does not dip to very low as like HAZ (Fig. 6). This is due to the work hardening effect of pin [21]. Post weld tensile strength of the material depends on the change in the hardness of it during the process. So peak process temperature cannot be raised beyond a point which results in too much reduction of hardness of material in HAZ. Fig. 8 explains the reduction in hardness value with respect to the temperature rise in HAZ. Fig. 8 was constructed based on the minimum hardness values extracted from various trials shown in Fig.6. It can be observed that there is sudden drop in the slope after 425 in Fig. 8. It reveals that if the temperature is increased beyond this cut-off point (425) in HAZ, it drastically eradicates the post weld properties of the joint. This is due to the coarsening of grains which reduces the concentration of strengthening agents [22]. So peak process temperature cannot be raised beyond a point which results in temperature rise of more than 425 although it assists in the reduction of stress on the tool pin.

5.2 Estimation of principal stress

Stress on the tool pin increases from the root and it attains its maximum value at the tip of the pin. Unlike circular pins, the non-uniform contact boundary distance from the rotational axis of triangular and square shapes create variation in stress along the edges of the pin. Fig. 9 represents the variation in maximum amount of stress due to bending and shear experienced by the tool pin with respect to the process temperature. These values were estimated through he analytical Eqns.16-21. Stress on the tool pin is created by the opposing force induced by the temperature dependent strength of the material handled by the pin in the SZ. Fig. 9 shows the variation of maximum stress created by the strained material in the SZ. It can be observed that the value of stress is comparatively very less for the square shaped pin in every level of process temperature. When the process peak temperature reaches solidus temperature of the material the shear stress reaches a very low value of 50Mpa as the material loses its strength completely and it tends to become liquid.

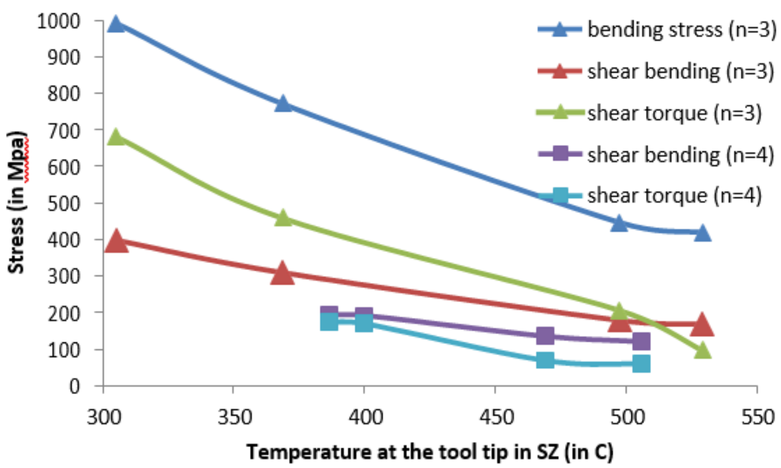

Fig. 9 - Variation in stresses with respect to process peak temperature

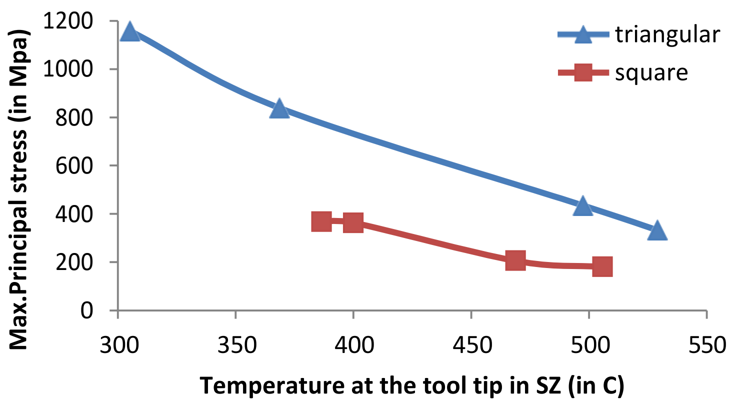

Fig. 10 - Variation in Principal stress with respect to process peak temperature

Based on the process temperature, variation in principal stress created by the combined effect of normal bending stress, shear bending stress and shear torque are shown in Fig. 10. Fluctuations in the maximum principal stress depend on every single parameter listed in Table 4. So the simple way to quantify its variation is through its corresponding process temperature which depends on all the chosen parameters for the trial. As expected when the temperature increases, principal stress on tool pin reduces (Ref. Fig. 10). Computed values of maximum stress denote that square shaped pin experiences less stress than triangular shaped pin and difference increases when the process temperature reduces. For the square shaped pin profile, it has been estimated that the normal bending stress is zero at the point where maximum principal stress exists (Ref. Eqn. 19). But in this point, shear stress due to bending and torque are aligned to each other ($\beta = 0^{\circ}$) as shown in Fig.3 and this exhibits higher impact on the rise of principal stress at this point. Reduction on maximum principal stress with respect to increase in the number of sides in the pin denotes the structural stiffness of square shape against the traverse force exhibited by the material in SZ.

5.3 Statistical estimation

Estimation of stress on tool pin needs an empirical model which correlates to the major impact variables listed in Table 4. From Fig. 9 & 10, it is understood that estimation of temperature is the simplest way to estimate the stress on the tool pin. As the temperature rises based on the different levels of process, parameters are identified accurately, obtaining a correlation for temperature rise with the major impact process parameters that can assist to quantify stress with respect to the selected process parameters.

From the analytical models, it is clear that,

$$\tau_{max} = f(\sigma_b, \tau_b, \tau_t)$$
$$\sigma_b, \tau_b, \tau_t = f(a, H_{pin}, \tau(t))$$

Process temperature $T = f(Q_{Total}$, heat diffusion in the material, boundary conditions)

Considering the analytical equation on the estimation of total heat generation (Eqn. 23), it can be concluded that the major factors that affect the process thermal history are tool shape, dimension, vertical pressure, tool rotational speed and weld velocity.

So, Process peak temperature raise,

$$T = f(R_{Shoulder} / R_{Pin}, \omega / V, P, n) \tag{24}$$

In this equation temperature response is a function of four variables and graphical representations are not possible. So following expression is formed through multiple regression analysis using direct method.

$$T = a + b_1(P) + b_2(\omega / V) + b_3(R_{Shoulder} / R_{Pin}) + b_4(n) \tag{25}$$

Here, a is the intercept, b_1, b_2, b_3 and b_4 denotes the expected change in temperature response per unit change in vertical force, rotational speed per feed rate, ratio between shoulder & pin radius and number of flat faces in the pin respectively. With respect to the chosen variables in Table.4 and corresponding temperature responses represented in Fig. 7, constants in the Eqn. 25 is estimated and listed in Table 6.

Table 5 - Summary output

Regression Statistics	
Multiple R	0.950 641
R Square	0.903 718
Adjusted R Square	0.868 706
Standard Error	23.72 112
Observations	8

Table 6 - Regression analysis data

	Coefficients
Intercept	-149.608
Vertical force	23.85692
Heat index	3.399858
R(shoulder) / R(pin)	45.66784
n	7.235864

Applying the coefficient obtained through regression analysis, empirical model for temperature response can be written as,

$$T = -149.08 + 23.857\ (P) + 3.4\ (\omega / V) + 45.67\ (R_{Shoulder} / R_{Pin}) + 7.236\ (n) \quad (26)$$

R square value in the output summary denoted in Table 5 reveals the accuracy level of usage of this temperature response model. Based on this correlation, temperature response lines can be drawn for different levels of process variables and as the tool index is the direct function of process temperature in the SZ, these temperature lines can be interpreted as tool index line using the relationship between temperature rise and tool index.

5.4 Optimisation of minimum and maximum limits of process domain

Increase in process temperature in the SZ reduces the stress on the tool pin. But this affects the post weld properties of the weld in the HAZ as shown in Fig. 6. So it is a must to limit the level of process parameter in such a way that it should not generate heat which is high enough to reduce the strength of the material in HAZ. It has been observed from Fig. 8 that when the temperature reaches 425, it produces structural changes which reduce the hardness of the material in HAZ. This effect is limited in SZ by the strain hardening effect. This indicates that the maximum process temperature in SZ should be selected in such a way that it should not result a temperature rise of more than 42 in HAZ. To identify this maximum limit a graph is drawn (Fig. 11) between the maximum temperature in SZ and it corresponding maximum temperature rise in HAZ. From Fig.11 it has been estimated that temperature in SZ cannot be increased more than 470 during the usage of triangular pin profile and 460 during the usage of square pin profile.

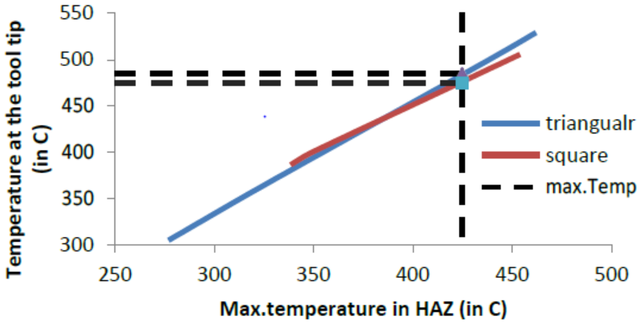

Fig. 11 - Maximum temperature response in HAZ for the process peak temperature in S

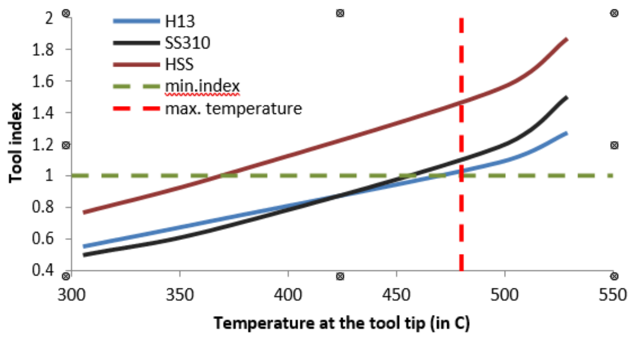

Fig. 12 - Estimated tool index for triangular pin for different tool materials

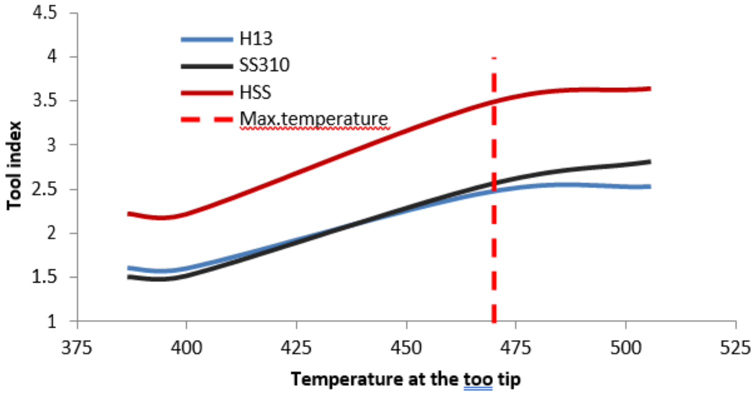

Fig. 13 - Estimated tool index for square pin for different tool materials

Elevated temperature in the tool/matrix interface not only affects the strength of the strained material but also reduces the strength of the tool. The ratio between the maximum stress acting on the tool and the strength of the tool at the operating temperature delivers a quantitative measurement of tool durability. For the current analysis, commonly used low strength tool materials tool steel (H13), SS310 and high speed steel (HSS) are considered as the joining process is carried out for AA2024-T3. The computed results for triangular and square pin profiles are shown in Fig. 12 and Fig. 13 respectively. As expected reduction in process temperature increases the stress acting on the tool pin and in turn reduces the tool durability. Hardness test results shown in Fig. 8 suggest to maintain the peak process temperature as minimum as possible to enhance post weld property of the joint. But reducing temperature in the SZ results tool index number lesser than 1 on the usage of triangular shape pin profile in the tool (Fig. 12). Especially usage of low strength material like H13 and SS310 in the tool, operating temperature cannot be reduced less than 450 for triangular pin profile. Even when the chosen pin shape is square, its index value is closer to 1 in lower working temperature levels (Fig. 13). So, minimum limit of the process domain has to be fixed based on temperature rise of 450 on the usage of triangular pin profile which can be reduced up to 400 on the usage of square pin profile. On the other hand, temperature in SZ cannot be increased beyond 470 to enhance tool durability at the cost of post weld joint strength. So, maximum limit of process domain can be fixed based on 470 temperature rise in SZ. Usage of HSS as tool material in the tool with triangular pin exhibits a considerable improvement in tool index even at lower temperature and reduces the lowest process temperature limit up to 400. This suggests that high strength materials like tungsten based alloys or PcBn martial should be opted as tool material for triangular pin profile.

5.5 Tool durability chart based on optimised process domain

Based on the quantitative relation between the maximum temperature in SZ and tool index shown in Fig. 12 & 13, the obtained empirical relationship (Eqn. 26) can be used to develop tool index lines with respect to the process variables. Tool index for different tool materials with respect to the maximum temperature for the chosen process variables are shown in Table 7. Using this relationship statistically attained temperature response lines are interpreted as tool index lines for different tool materials as shown in Fig. 14 & 15 relate the major controllable process parameters with tool index.

Table 7 - Estimated tool index for different experimental trails

Trail No.	Max.Temp (C)	Lowest HV	Max.Principal stress (Mpa)	Tool index		
				H13	SS310	HSS
1	305.2	111.8	1157.928	0.548833	0.49473	0.765862
2	368.63	109.64	838.724	0.722204	0.667681	0.998
3	497.43	104.6	434.8317	1.083135	1.182242	1.550245
4	528.94	102.23	332.5758	1.271476	1.49981	1.869054
5	386.49	109.64	368.6715	1.608448	1.505994	2.222588
6	399.83	107.86	363.5595	1.601455	1.516427	2.214732
7	505.74	103.3	181.3294	2.469509	2.552317	3.47743
8	468.85	105.74	206.3059	2.530586	2.813675	3.64383

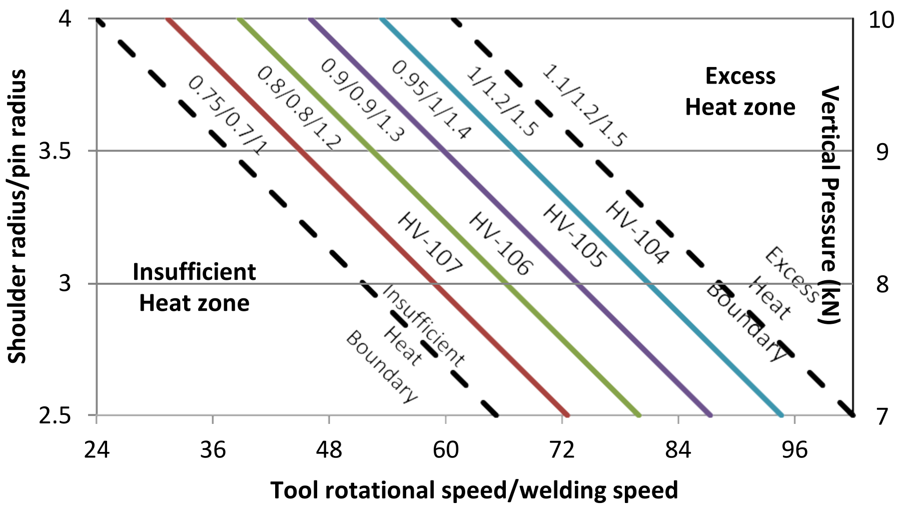

Fig. 14 - Durability chart for tools (H13/SS310/HSS) with triangular pin

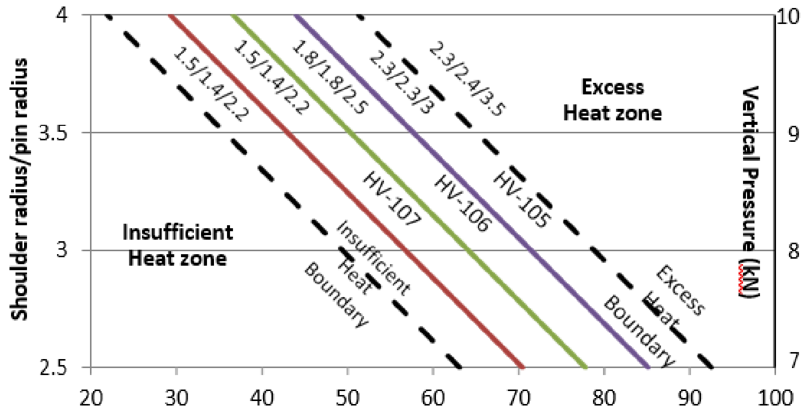

Fig. 15 - Durability chart for tools (H13/SS310/HSS) with square pin

From the previous analysis it is understood that the process temperature cannot be reduced lesser than 400 to enhance the post weld properties as the tool index is reduced less than 1. At the same time, process temperature cannot be increased more than 470 as it affects the post weld properties of the joint for triangular pin profile. Similarly the process peak temperature range for the square pin is optimised between 400 and 460. Based on this temperature range, domain tool index charts are prepared as shown in Fig. 14 & 15 for triangular and square pin profile respectively. These charts assist on proper selection of process variables based on the requirement. For instance, on the usage of soft tool materials combination of process variables can be chosen with the reference of higher value tool index lines. On the other hand, if tools are made with higher strength materials, lower value index lines can be chosen to enhance the post weld properties of the joint. Apart from this, the possible post weld lowest hardness value of AA2024-T3 joints on the selection of process parameters with the reference of every line is denoted in the chart to predict the quality of the weld. This facilitates more flexibility on the usage of this chart based on the application. Especially AA2024-T3 is widely used in aerospace industries where priority is given to the post weld properties and low tool index lines can be the reference lines. Higher value tool index lines can be opted for other applications with the permissible limit of compromise in weld quality to improve tool life.

6. Conclusions

Tool durability depends on temperature dependent material properties of tool as well as the metal to be joint. Temperature gradients developed on the selection of various levels of process parameters were estimated in stir zone using numerical model. Obtained results were validated through experimental analysis. A novel analytical model to estimate torque developed by the flat surfaces of the tool pin was derived. Using this, existing temperature dependent analytical model to estimate maximum principal stress was remodified. This remodified analytical model improved the accuracy on predicting maximum stress for triangular and square tool pin profiles. Effects of temperature rise on post weld material properties were identified using hardness analysis at various points in stir as well as heat affected zones. Based on the results obtained on the joining process of AA2024-T3, it was concluded that,

- Although the increasing temperature in stir zone improves tool durability, it affects the material property in the heat affected zone during the process. So the maximum possible raise of temperature is 460 and 470 on the usage of square and triangular tool pins respectively.

- Reducing process peak temperature could improve post weld properties of the material in heat affected zone. But on the other hand it affects tool life as the strength of material strained by the tool in stir zone increases. So process temperature cannot be reduced less than 400 which leads to premature tool failure.
- Although the process was carried out in the optimised temperature domain, usage of soft materials like H13 and SS310 in the tools with triangular pin profile is not recommended as the maximum tool index number could not be raised more than 1 even the joining process was carried out in the highest temperature domain limit.

With the reference of optimised temperature domain, durability maps were prepared for the tools with triangular as well as square pin profiles. As the tool index lines are prepared with the reference of process peak temperature, the possible lowest post weld hardness value of the joint is also mentioned in the chart. So reference lines in the charts for the selection of process variable in the chart not only assist the user to predict the tool life but it also forecasts the possible degradation of material properties in the heat affected zone.

References

[1] Samir Sani Abdulmalik, Rosli Ahmad, (2018). Influence of Friction Stir Process on Microstructure and Tensile Properties of LM28 Hypereutectic Al-Si Alloy, International Journal of Integrated Engineering, 10(3), 63-68

[2] Md Reza-E-Rabby, Wei Tang, Anthony P Reynolds, (2018). Effects of thread interruptions on tool pins in friction stir welding of AA6061, Science and Technology of Welding and Joining, 23(2), 114-124

[3] Shubham Verma, Meenu Gupta, Joy Prakash Misra, (2019). Effect of pin-profiles on thermal cycle, mechanical and metallurgical properties of friction stir–welded aviation-grade aluminum alloy, Proceedings of the Institution of Mechanical Engineers, Part B: Journal of Engineering Manufacture, 233(11), 2183-2195

[4] Mishra R S, Mahoney M W, Ed., (2007). Friction Stir Welding and Processing, ASM International. ISBN: 978-0-87170-840-3

[5] Mahoney M.W., Bingel W.H., Sharma S.R., Mishra R.S., (2003). Microstructural modification and resultant properties of friction stir processed cast NiAl bronze, Materials Science Forum, 426 – 432

[6] Aissani M., Gachi S., Boubenider F., Benkedda Y., (2010). Design and optimization of friction stir welding tool, Materials and Manufacturing Processes, 25 (11), 1199 – 205

[7] M.Felix Xavier Muthu, V.Jayabalan, (2016). Effect of pin profile and process parameters on microstructure and mechanical properties of friction stir welded Al–Cu joints, Transactions of Nonferrous Metals Society of China, 26 (4), 984-993

[8] Thomas W.M., Lockyer S.A., Kalee S.W., Staines D.G., (2003). Friction stir welding: an update on recent developments, Proceedings of the Conference on Stressed Components in Aluminium Alloys , Birmingham, UK

[9] Thomas W.M., Johnson K.I., Wiesner C.S., (2003). Friction stir welding recent developments in tool and process technologies, Advanced Engineering Materials, 5 (7), 485-90

[10] Colegrove PA., Shercliff HR., (2006). CFD modeling of friction stir welding of thick plate 7449 aluminium alloy. Science and Technology of Welding and Joining. 11, 429-41

[11] Vijay S.J., Murugan N., (2010). Influence of tool pin profile on the metallurgical and mechanical properties of friction stir welded Al–10 wt. % TiB2 metal matrix composite, Materials & Design,. 31, 3585-3589

[12] Gadakh V.S., Kumar A., (2014). Friction stir welding window for AA6061-T6 aluminium alloy, Proc IMechE, Part B: J Engineering Manufacture, 228(9), 1172-1181

[13] A. Arora, M. Mehta, A. De, T. DebRoy, (2012). Load bearing capacity of tool pin during friction stir welding, International Journal of Advances in Manufacturing Technology, 61, 911-920

[14] M.Mehta, G.M.Reddy, A.V.Rao, A.De, (2015). Numerical modeling of friction stir welding using the tools with polygonal pins, Defence Technology, 11, 229-236

[15] Ashish Bist, J.S.Saini, Bikramjit Sharma, (2016). A review of tool wear prediction during friction stir welding of aluminium matrix composite, Transactions of Nonferrous Metals Society of China, 26(8), 2003-2018

[16] Arora A., De A., DebRoy T., (2011). Toward optimum friction stir welding tool shoulder diameter, Scripta Materialia. 64, 9-12

[17] Li Q., Lovell M., (2005). On the critical interfacial friction of a two-roll CWR process, Journal of Materials Processing Technology, 160, 245-256

[18] M. Mehta, A. Arora, A, T. DebRoy, (2011). Tool geometry for friction stir welding – optimum shoulder diameter, Metallurgical and Materials Transactions A. 42A(9), 2716–2722

[19] Igor Zybin, Konstantin Trukhanov, Andrey Tsarkov, Sergey Kheylo, (2018). Backing plate effect on temperature controlled FSW process. MATEC Web of Conferences, 224: 01084

[20] L.Shi, C.S.Wu, (2017). Transient model of heat transfer and material flow at different stages of friction stir welding process, Journal of Manufacturing Processes, Journal of Manufacturing Processes, 25, 323-339

[21] Zhixiong Zhu, Jian Han, Chong Gaob, Mao Liud, Jianwei Song, Zhiwei Wang, Huijun Li, (2017). Microstructures and mechanical properties of Al-Li 2198-T8 alloys processed by two different severe plastic deformation methods: A comparative study, Materials Science & Engineering A, 681, 65-73

[22] Djarot B. Darmadi1, Annisha Mentary, E.M. Yusup, S. Mahzan, (2019). Evaluating The Effect of The Pin's Length to The Strength of Double Sides Friction Stir Welded Aluminum, International Journal of Integrated Engineering, 11(5), 1-11